PCCP

PAPER

View Article Online
View Journal | View Issue

Cite this: *Phys. Chem. Chem. Phys.*, 2018, **20**, 10949

Intramolecular vibrational energy redistribution in $HCCCH_2X$ (X = Cl, Br, I) measured by femtosecond pump–probe experiments in a hollow waveguide

Alexander Kushnarenko, Eduard Miloglyadov, Martin Quack * and Georg Seyfang

From the analysis of high resolution overtone spectra it is well established that intramolecular vibrational energy redistribution (IVR) from an initially excited CH-stretching vibration is strongly influenced by its chemical environment. Due to a pronounced Fermi resonance between the CH-stretching and CH-bending vibrations a vibrational energy redistribution on the subpicosecond time scale (~100 fs) is found for alkyl (sp^3) CH-chromophores, whereas this doorway for energy flow is blocked for the acetylenic (sp) CH-stretching vibration because of the much lower CH-bending frequency. From the analysis of the high resolution spectra lifetimes for the initial CH-vibrational excitation of 10–100 ps or longer have been derived. In the present work we have investigated the IVR process for $HCCCH_2Br$, $HCCCH_2Cl$, and $HCCCH_2I$ after excitation of the first overtone of the CH-stretching vibration of the CH_2X- and the CCH-group by time resolved femtosecond pump–probe experiments in a hollow waveguide. For $HCCCH_2Br$ and $HCCCH_2Cl$ a clearly different IVR behavior was found for the two different chemical environments. For the excitation of the alkyl CH-chromophore very fast initial relaxation times were found together with a slower relaxation process with τ_2 = 15–40 ps, whereas for the acetylenic CH-stretching vibration a relaxation time τ_3 = 70–200 ps has been determined. For $HCCCH_2I$ also for the excitation of the CCH-group a relatively fast relaxation process with a time constant τ_2 = 6 ps could be identified which might result from a not yet identified strong vibrational coupling between the excited first overtone of the acetylenic CH-stretching vibrations with a combination state including the CI-stretching vibration.

Received 21st December 2017,
Accepted 6th March 2018

DOI: 10.1039/c7cp08561c

rsc.li/pccp

1 Introduction

Intramolecular vibrational energy redistribution (IVR) is of fundamental importance in physical chemistry. It is a central aspect for statistical reaction rate theories where it is assumed that redistribution proceeds faster than reaction such that microcanonical intramolecular equilibrium is reached prior to reaction.[1–10] The question concerning the time scale of IVR received further importance when the first IR-multiphoton experiments indicated that a mode selective chemistry can only be expected if the unimolecular reaction step at a certain excitation energy is faster than the IVR process.[11–19]

Given the understanding from the early days of molecular quantum dynamics, that anharmonic resonances leading to IVR can be quantified by stationary state spectroscopy,[20,21] the fundamental questions on the kinetics of IVR resulted in a major effort to derive the underlying quantum dynamical process from highly resolved spectra starting in the early 1980s.[22–34] In this approach in essence one derives the solution of the time dependent Schrödinger equation (1) and (2)

$$i\frac{h}{2\pi}\frac{\partial\Psi(q,t)}{\partial t} = \hat{H}\Psi(q,t) \quad (1)$$

$$\Psi(q,t) = \hat{U}(t,t_0)\Psi(q,t_0) \quad (2)$$

from the analysis of the high resolution spectra related to the stationary state Schrödinger equation

$$\hat{H}\phi_k(q) = E_k\phi_k(q) \quad (3)$$

leading to one possible solution for $\Psi(q,t)$

$$\Psi(q,t) = \sum_k c_k\phi_k(q)\exp(-2\pi i E_k t/h), \quad (4)$$

where q represents the whole set of relevant generalized coordinates of the constituents of the molecule. One can derive other forms of the solution in terms of the time evolution operator $\hat{U}(t,t_0)$ if, for instance, electric dipole interaction with a time dependent

ETH Zurich, Lab. für Physikalische Chemie, HCI E235, Vladimir-Prelog-Weg 1-5/10, 8093 Zurich, Switzerland. E-mail: Martin@quack.ch; Fax: 41 44 632 10 21; Tel: 41 44 632 44 21

electromagnetic field is included, where the relevant electric (or magnetic) dipole matrix elements are derived from spectroscopic intensities (see ref. 12, 14, 18, 30 and 32 for example).

One might call this approach "kinetics in the imaginary world", given the important imaginary contribution to these solutions for $\Psi(q,t)$ (with $i = \sqrt{-1}$ in these equations). There has been some debate, whether this approach leads to comparable results as the time resolved kinetics experiments, say by femtosecond pump–probe spectroscopy in the "real world".[32,35–38] In particular there has been some discussion about one striking finding derived from the stationary state spectroscopy approach: the initial IVR times with overtone excitation of the alkyl (sp^3 hybridized) CH-chromophore are typically about 100 fs, whereas the initial decay with overtone excitation of the acetylenic (sp hybridized) ≡C–H-chromophore are found in the range 10 to 100 ps or even longer, thus on a time scale contradicting a dogma of early statistical theories requiring subpicosecond equilibration typically (see ref. 16 and 22–34 for some summaries and early reviews).

Here we address this question by the time dependent "real world" approach in femtosecond or picosecond pump–probe experiments. In this approach the CH-stretching vibration or its overtone is excited by a strong pump pulse and after a certain delay time the progress of intramolecular vibrational energy redistribution is determined through the absorption of a weak second IR-pulse,[39–43] a UV-pulse[44–52] or the relaxation of the molecules is detected in a (1 + 1) resonantly enhanced multiphoton ionization (REMPI) process.[53,54] In the UV-probing the time evolution of the absorption cross section is measured directly, whereas the (1 + 1)-REMPI signal is proportional to the absorption cross section of the first step.[53,54] The UV- and REMPI-probing makes use of the finding that the UV-absorption spectra of vibrationally excited molecules in general are broadened and shifted to longer wavelengths after intramolecular vibrational relaxation, as usually there is no or only negligible Franck–Condon overlap to the electronically excited state for the initially excited CH-stretching vibrational state. For this detection method the spectral change of the UV-spectrum and the absorption of the probe pulse indicates the progress of the IVR process. In some cases, as in CH_3I, the change of the UV-spectra is directly correlated with the time averaged population of a single vibrational mode.[55,56]

In the present work we have chosen to investigate bichromophoric propargyl halides as it can be assumed that the change of the UV-spectra is connected in a similar manner to the population of the CX-stretching vibration. At the same time one finds both the sp^3-CH chromophore and the sp-CH chromophore in the same molecule thus the kinetics with the excitation of either chromophore can be studied, all other things being equal (see Fig. 1). Due to the anharmonic shift in the excited vibration, the population of the initially excited mode can be followed directly by probing in the infrared and the decay process from the initially excited vibrational states is obtained. On the other hand, UV-probing allows for a measurement of the kinetics of the transfer of energy to the C–X-vibrations.

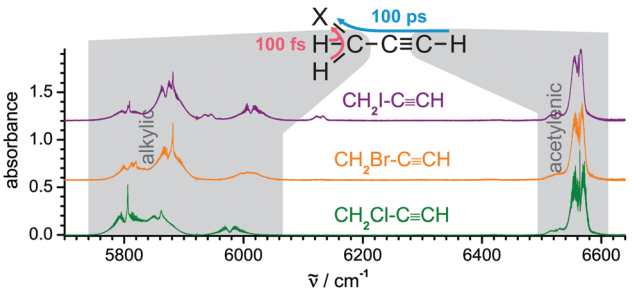

Fig. 1 IR-spectra for $HCCCH_2Cl$ (lower trace), $HCCCH_2Br$ (middle trace) and $HCCCH_2I$ (upper trace) in the region of the first overtone measured with an instrumental bandwidth of 5.5×10^{-3} cm^{-1} on our FTIR-spectrometer (Bruker HFS125, Zürich prototype ZP2001) with an optical path length of 19.2 m and a gas pressure of 200 Pa. The baselines for the decadic absorbance $lg(I_0/I)$ shown are shifted by 0.6 for $HCCCH_2Br$ and by 1.2 for $HCCCH_2I$ for better visibility in this survey. The shaded areas indicate the idealized bandwidths of the femtosecond laser pulses of the excitation laser. The times shown for the kinetics indicate the main aspects semi-quantitatively.

The process of intramolecular vibrational energy redistribution after excitation of the fundamental of the acetylenic CH-stretching vibration has been already investigated by picosecond IR-IR pump–probe experiments for $HCCCH_3$, $HCCCH_2F$, and $HCCCH_2Cl$,[57] which provides a good starting point for our study, see also ref. 58 and 59. These molecules were excited at 3330 cm^{-1} and probed at the shifted $\nu_1 = 1$ to $\nu_1 = 2$ vibrational transition at 3025 cm^{-1}. In the analysis of the decay process a two step mechanism was assumed: first a relaxation from the initially excited CH-stretching vibration to two quanta in the acetylenic CH-bending mode which is followed afterwards by the process leading to complete relaxation. For $HCCCH_2F$ and $HCCCH_2Cl$ the depopulation of the initially excited CH-stretching vibration could be represented by a first order decay process with a relaxation time $\tau_1 = 89$ ps for the fluoride and $\tau_1 = 380$ ps for the chloride. For propyne a more complicated decay process with $\tau_1 = 32$ ps and $\tau_2 = 520$ ps was found and it was stated that the IVR process was limited to states with high K rotational quantum numbers where a Coriolis coupling might become important. Due to the high pressure and the slow relaxation process collisional effects could not be excluded in these earlier experiments[57] (see also ref. 60–62).

In the present experiments we have excited the first overtone of the alkylic and acetylenic CH-stretching vibration around 6000 cm^{-1} and 6550 cm^{-1} respectively for $HCCCH_2Cl$, $HCCCH_2Br$ and $HCCCH_2I$. The progress of the IVR process was followed by time resolved, sensitive UV- and IR-absorption spectroscopy. The UV-detection is based on the experimentally and theoretically well established finding that the excited CH-stretching vibrational states in the electronic ground state show unfavourable Franck–Condon factors to the electronically excited states with no vibrational excitation in CH-stretching. Only after redistribution of the vibrational energy to the low lying C–X-vibrational modes a shift of the absorption spectrum to longer excitation wavelengths is observed. For the IR-probing the vibrational population directly (if the upper level of the probed transition is not populated) or the population difference between two levels (if both levels are

populated) are obtained. In the set up of our experiment we increased the interaction length for the absorption and to improve the probe signal the pump- and the probe-beam are coupled into a waveguide of L_{wg} = 500 mm.[52,63,64] A clearly different IVR kinetics was found for the excitation of the CH-stretching vibration at the CH_2X-group as compared to excitation at the CCH-group. Fig. 1 summarizes the structures of these bichromophoric molecules, their survey spectra in the excited wavenumber ranges and anticipates the main kinetic results in a simplified survey.

In Section 2 we describe the experimental approach in some detail. Section 3 contains the experimental results for the time dependent kinetics with IR and UV-probing. The difference in the decay function for the two spectral probing ranges is explained and their consequences for the interpretation of the IVR process are discussed. We conclude with a detailed discussion in Section 4. Some preliminary results of our work were reported in ref. 65 and 66.

2 Experimental

2.1 Pump–probe experiments with time-resolved UV-detection

A schematic view of our experimental setup is shown in Fig. 2. Laser pulses at 795 nm with a pulse energy of about 1 mJ and a pulse length of 150 fs are generated at a repetition rate of 1 kHz in a femtosecond Ti:Sapphire oscillator–regenerative amplifier system (Clark MXR, Model CPA-1000). In a later stage of the experiment the Ti:Sapphire oscillator has been replaced by a fiber laser (Menlo-Systems, T-Light). The output beam of the amplifier is divided by a beam splitter BS1 (R = 60%) to pump two identical travelling wave optical parametric generators OPG-1 and OPG-2 (TOPAS, Light Conversion). From OPG-1 near-IR laser pulses from 4000 to 9000 cm^{-1} (idler or signal) with a pulse energy of up to 60 μJ are obtained and from OPG-2 the fourth harmonic of the signal wave is generated in two BBO crystals to produce UV laser pulses of up to 5 μJ in the spectral range 27 500–32 500 cm^{-1}. To obtain UV light up to 42 000 cm^{-1} the output of the fourth harmonic of OPG-2 is mixed with the residual light of the pump beam in an additional BBO crystal. The spectral widths of the near-IR pump pulse and of the UV probe pulse are determined by the spectral width of the Ti:Sapphire oscillator and are measured to be 120–150 cm^{-1}. For the IR-probing the second/fourth harmonic generation is replaced by difference frequency generation of the signal and idler wave of OPG-2 in a $AgGaS_2$-crystal (Light Conversion).

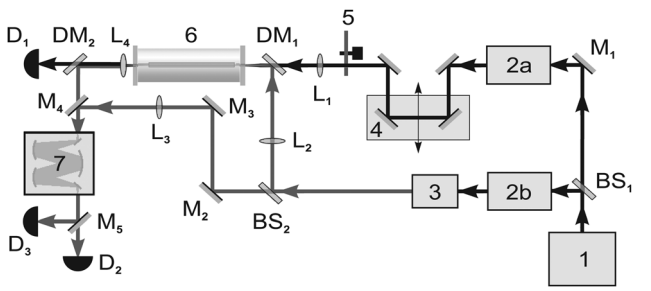

Fig. 2 Experimental set-up with the abbreviations: 1: Ti-Sapphire laser system, 2a, b: optical parametric generator, 3: higher harmonic generator (UV-detection) or difference frequency generation (IR-detection), 4: delay line, 5: chopper, 6: absorber cell with optical waveguide, 7: monochromator for enhanced resolution (IR-detection only), M1–M5: mirror, BS1,2: beam splitter, L1–L5: lenses, DM1,2: dichroic mirrors for the combination and separation of pump- and probe beam, D1–D3: detectors.

To measure the time evolution of the UV-absorption after overtone excitation the near-IR pulses are sent through a variable delay line with a maximum delay time of 1000 ps. The laser beams are focused with lenses of f_1 = 150 mm (near-IR) and f_2 = 200 mm (UV, IR) respectively to the entrance opening of a fused silica hollow waveguide of inner radius a = 125 μm and a length of L_{wg} = 500 mm. The waveguide is mounted into a glass cell with fused silica windows and the two beams are overlapped on a beam splitter in front of the cell. The focal lengths of the focusing lenses are chosen to match the beam diameter ω of the free laser beams to the inner diameter of the waveguide (for details see below).

To measure sensitively the IVR process initiated by the near-IR pump light and to obtain its influence on the transmitted probe light the output from the near-IR OPG1 is modulated by an optical chopper at a frequency of 1/4 of the pump laser repetition rate. The relative pulse energy of the UV-beam is measured for every laser pulse before and behind the sample cell on two photodiodes D2 and D3 respectively, while the transmitted near-IR light is sent to the detector D1. To reduce effects from stray light, for the UV-detection GaP-photodiodes (Hamamatsu G1962) with a long wavelength cut-off at 500 nm are used for D2 and D3 and a near-IR sensitive InGaAs-photodiode (Hamamatsu G5832) for D1. To remove parasitic light at other wavelengths separating prisms are put in front of the detectors. To increase the spectral selectivity and to suppress stray light of our IR-detection scheme the probe light (transmitted and reference beam) was sent through a monochromator (Jobin-Yvon H25). The slits of the monochromator were chosen such as to allow for a spectral width of 3–5 cm^{-1} for the transmitted light. The beam transmitted through the probe cell and the reference beam were sent behind the monochromator to two identical PbSe-detectors D2 and D3.

The signals from the different detectors are sent to a fast data acquisition card (National Instruments, PXI-6115, 12 bit, 10 MHz sampling rate). After transfer of the data to the computer the response curves of the different detectors were integrated to obtain the relative pulse energy S_{Di} and the difference of the ratio S_{D2}/S_{D3} when the pump laser is on minus the ratio when the pump laser is off is calculated to obtain the time dependent UV-absorption signal

$$\Delta^{n}_{pr} = \frac{S_{D2}/S_{D3}(\text{near-IR on}) - S_{D2}/S_{D3}(\text{near-IR off})}{S_{D2}/S_{D3}(\text{near-IR on}) + S_{D2}/S_{D3}(\text{near-IR off})} \quad (5)$$

Typically 3000–5000 laser pulses were added for each delay time and 3–5 different experiments were averaged for every decay function.

The temporal shape of the laser pulses has been determined measuring the correlation function for the second harmonic

generation of the pump pulse in a BBO crystal or the sum frequency generation of the pump with the probe pulse for the UV-probing in a BBO crystal, and for the IR-probing in a KTP crystal. Depending on the master oscillator of the Ti:Sapphire laser and the alignment of the compressor pulse lengths between 140 and 190 fs have been obtained. The spectral distribution of the laser pulses was measured using a Czerny–Turner type monochromator (Jobin-Yvon H25). The laser pulses were found close to Fourier limited for a Gaussian distribution. No significant increase of the laser pulse duration was found sending the laser pulse through the empty or gas filled capillary (see below). From this we conclude that the 150 fs time resolution is effectively maintained.

2.2 Improved sensitivity in a hollow waveguide

We have shown previously that hollow waveguides are an excellent technique for pump–probe experiments in the gas phase to increase the effective interaction volume of two high intensity laser beams and to improve the signal-to-noise ratio.[52,63,64] In femtosecond pump–probe experiments the measured probe signal is determined by the overlap integral of the fluence distributions of the pump beam $F_{\mathrm{pump}}(x,y,z)$ and $F_{\mathrm{probe}}(x,y,z)$ of the probe beam and the product of the absorption cross section σ_{pump} at the wavelength of the pump beam and σ_{probe} at the wavelength of the probe beam:

$$\begin{aligned} \Delta_{\mathrm{UV}} &= U_{\mathrm{D}}(\text{pump on}) - U_{\mathrm{D}}(\text{pump off}) \\ &\propto \sigma_{\mathrm{pump}} \cdot \sigma_{\mathrm{probe}} \cdot C \iiint F_{\mathrm{pump}} \cdot F_{\mathrm{probe}} \cdot \mathrm{d}x \cdot \mathrm{d}y \cdot \mathrm{d}z. \end{aligned} \tag{6}$$

The coupling of a Gaussian laser beam to a cylindrical hollow waveguide is well understood theoretically[67,68] and experimentally as well.[52,69] Due to the cylindrical symmetry of the linearly polarized Gaussian laser beam only the HE_{1m}-modes are excited in the waveguide and the radial intensity distribution can be approximated for the limiting case $\lambda \ll a$ (laser wavelength λ, inner radius of the waveguide a) by a zero-order Bessel functions of the first kind $J_0(u_m r/a)$, u_m being the m-th root of the zero-order Bessel function. For a given wavelength the coupling efficiency and the intensity distribution within the waveguide are completely determined by the ratio of the Gaussian beam waist ω to the inner radius a of the waveguide, as can been seen from eqn (7), describing the coupling efficiency of the Gaussian laser beam to the waveguide mode m:

$$\eta_m = \frac{\left[\int_0^a \exp\left(-r^2/\omega^2\right) \cdot \mathrm{J}_0(u_m r/a) r \mathrm{d}r\right]^2}{\int_0^a \exp(-2r^2/\omega^2) \int_0^a \mathrm{J}_0^2(u_m r/a) r \mathrm{d}r}. \tag{7}$$

For a ratio $\omega/a = 0.64$ the coupling efficiency to the HE_{11} mode is more than 98% as was shown experimentally in ref. 63. This is the optimum condition for pump–probe experiments in a hollow waveguide.

In addition to the coupling efficiency also dispersive properties of the hollow waveguide have to be considered.[67] Under our experimental conditions the losses of the UV-probe beam ($\lambda_{\mathrm{probe}} \simeq 310$ nm) in a waveguide of length $L_{\mathrm{wg}} = 500$ mm and an inner radius $a = 125$ μm are negligible whereas they are around 50% for the near-IR pump beam ($\lambda_{\mathrm{pump}} \simeq 1700$ nm). Dispersion effects may lead also to a pulse broadening, but for our laser pulse lengths of $\tau_{\mathrm{pulse}} = 150$ fs they are less than 5% and can be neglected.

To estimate the improvement of the sensitivity of pump–probe experiments in a hollow waveguide, the measured probe signal for a confocal geometry in a cell without waveguide has to be compared to the signal for the arrangement with the waveguide. From eqn (8) one can see that the ratio $\gamma_{\mathrm{enhance}}$ of the probe signal for the two arrangements is given by the ratio of the overlap integrals of the fluence distributions of the pump and probe beam. It is given in a cylindrical coordinate system:

$$\gamma_{\mathrm{enhance}} = \frac{\iint F_{\mathrm{wg}}\left(\lambda_{\mathrm{pump}}, r, z\right) \cdot F_{\mathrm{wg}}\left(\lambda_{\mathrm{probe}}, r, z\right) \cdot r \cdot \mathrm{d}r \cdot \mathrm{d}z}{\iint F_{\mathrm{conv}}\left(\lambda_{\mathrm{pump}}, r, z\right) \cdot F_{\mathrm{conv}}\left(\lambda_{\mathrm{probe}}, r, z\right) \cdot r \cdot \mathrm{d}r \cdot \mathrm{d}z}, \tag{8}$$

where $F_{\mathrm{wg}}(\lambda,r,z)$ is the laser fluence distribution for the case of a hollow waveguide in a cell. For the free space between the cell windows and the waveguide we assume a Gaussian fluence distribution and within the waveguide the fluence distribution is described by a Bessel function of the first kind (see above). $F_{\mathrm{conv}}(\lambda,r,z)$ is the distribution of the laser fluence for the case of a conventional coaxial scheme (confocal gaussian laser beams). For a capillary with a length of 500 mm and a inner diameter of 250 μm an enhancement factor of $\gamma = 10$ is calculated and has been verified experimentally.[63]

2.3 Experiments with spectral resolution in the IR

In the experiments the molecules are excited to the overtone of the CH-stretching vibration. The population in the $v_{CH} = 2$ vibrational level can be probed either in absorption to the $v_{CH} = 3$ vibrational level or in stimulated emission. Sending the probe beam through a monochromator the time evolution can be measured with a spectral resolution of 3–4 cm^{-1} using either a single InSb detector (Judson J10-D) or a HgCdTe-detector array (Hamamatsu P4249-9764, for details see in experimental set up corresponding diodes (arrays) D_2 and D_3).

With the infrared detection we are probing the initial part of the IVR dynamics, the relaxation of the initially excited $v_{CH} = 2$ vibrational state to the closely coupled isoenergetic background states. During the pump pulse a fast rise ($v_{CH} = 2 \rightarrow 1$ transition) or a fast decrease of the signal ($v_{CH} = 2 \rightarrow 3$ transition) is obtained which thereafter decays as a result of the IVR process. Due to the large anharmonicity of the CH-stretching vibration these two transitions are spectroscopically well separated. The decay process can be fitted by a sum of two exponential functions, resulting in two significantly different relaxation times around $\tau_2 = 10$ ps and $\tau_3 = 150$ ps for the excitation of first overtone of the acetylenic CH-stretching vibration. An example for the measured decay kinetics is shown for $HCCCH_2Cl$ in Fig. 3. The upper part of Fig. 3 shows the IVR kinetics measured with the detector array covering the spectral range from 3070 to 3280 cm^{-1} with a spectral resolution of approximately 4 cm^{-1} (to replace the detectors D2 and D3 in Fig. 2).

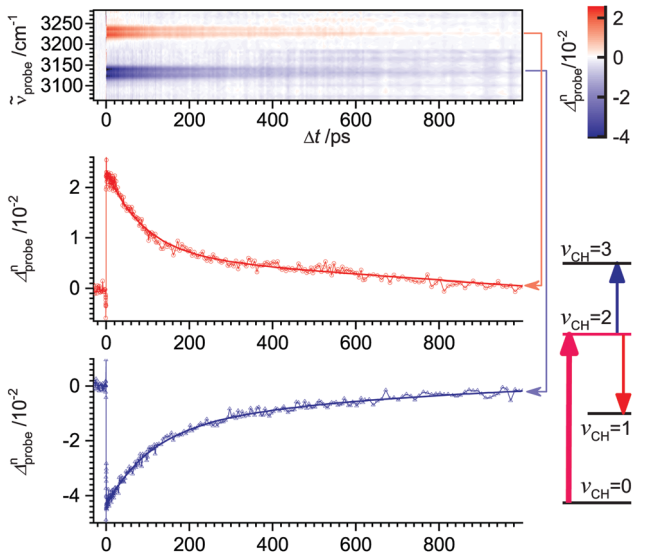

Fig. 3 Time evolution the variation of the transmitted IR probe signal after excitation of the overtone of the acetylenic CH-stretching vibration in $HCCCH_2Cl$ with a 150 fs laser pulse. On the right hand side of the figure the different molecular vibrational transitions are indicated by arrows (pink: excitation with the pump pulse to v_{CH} = 2, blue: absorption of the probe pulse on the v_{CH} = 2 → 3 transition, red: stimulated emission on the v_{CH} = 2 → 1 transition). The upper part of the figure shows the time evolution of the signal obtained from the detector array behind the monochromator (red: enhancement of the signal due to simulated emission, blue: reduction of the signal due to absorption). The two lower traces show the signal obtained from a single detector behind the monochromator at 3223 cm^{-1} (red, stimulated emission) and at 3141 cm^{-1} (blue, absorption). A sum of two exponential functions is fitted to the experimental decay curves resulting in two time constants τ_2 = 9 ps and τ_3 = 160 ps.

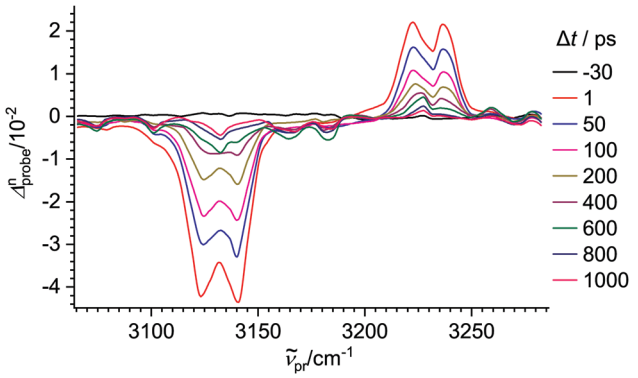

Fig. 4 Variation of the transmitted intensity of the IR probe pulse from 3050 to 3300 cm^{-1} after excitation of the overtone of the acetylenic CH-stretching vibration in $HCCCH_2Cl$ with a 150 fs laser pulse for different delay time between pump and probe pulse. As a result of the population of the v_{CH} = 2 vibrational level the signal decreases due to absorption on the v_{CH} = 2 → 3 transition and increases due to stimulated emission on the v_{CH} = 2 → 1 transition. As a result of IVR a reduction of the spectral variation with time is obtained.

If at certain time steps a cut is drawn through the signal recorded with the detector array a time dependent variation of the spectrum is obtained. The time evolution of the spectral variations is shown in Fig. 4, showing clearly the increase of the absorption on the v_{CH} = 2 → 3 vibrational transition around 3130 cm^{-1} and the stimulated emission on the v_{CH} = 2 → 1 vibrational transition around 3230 cm^{-1}.

2.4 Samples and their spectroscopic characterization

$HCCCH_2Cl$ was obtained from Sigma Aldrich (prepurified by destillation, bp. 331 K) and $HCCCH_2Br$ from ABCR chemicals (prepurified by destillation, bp. 362 K), $HCCCH_2I$ (bp. 388 K) was synthesized by Guido Grassi in our laboratory (following ref. 70). The compounds were analyzed by gas chromatography (GC) and further purified by GC, if necessary. The purity was estimated to be better than 98% for $HCCCH_2Cl$ and $HCCCH_2Br$ and better than 93% for $HCCCH_2I$ for our experiments. The identity of substances was obvious from the infrared spectra.

For the propargyl halides (point group C_s) there are two CH-stretching vibrations of the CH_2X-group, one with A′-symmetry (ν_2) around 2958–2976 cm^{-1} and one with A″-symmetry around 3005 cm^{-1} (ν_{11}), showing significantly lower intensity as compared to ν_2. The acetylenic CH-stretching vibration (A′, ν_1) is found at 3335 cm^{-1}.[71] For $HCCCH_2Cl$ and $HCCCH_2Br$ a relatively strong absorption around 2850 cm^{-1} has been identified as the overtone of the CH_2-bending vibration ν_4, indicating a strong resonance with the CH-stretching vibration ν_2. This Fermi resonance has been identified for a number of different compounds, but has not yet been analyzed in detail.[72]

In the overtone region between 5750–6600 cm^{-1} four different bands of significant intensity are found. Three arising from the overtone of the CH_2X-group at 5800, 5875 and 5980 cm^{-1} ($2\nu_2$, $\nu_2 + \nu_{11}$, $2\nu_{11}$) and one from the CCH-group at 6570 cm^{-1} ($2\nu_1$). The two bands from the combination of the two different CH-groups ($\nu_1 + \nu_2$ and $\nu_1 + \nu_{11}$), expected between 6200–6300 cm^{-1} could not be definitely identified in the spectra, as they are much weaker as compared to the other overtones. The spectra in the overtone region for the 3 different propargyl halides are shown in Fig. 1. For $HCCCH_2I$ two weak impurity bands appear at 5940 cm^{-1} and 6130 cm^{-1}. They are identified as overtones of the CH-stretching vibrations of iodoallene CHI═C═CH_2, arising from the thermal isomerization of propargyl iodide. The spectra in the overtone region of the acetylenic CH-stretching vibration are nearly identical for all the propargyl halides investigated. For $HCCCH_2Cl$ the *J*-structure of the rotational contour can be resolved whereas it is only barely resolvable for $HCCCH_2I$ due to its smaller *A* rotational constant. For all the compounds the hot band originating from the CCH-bending mode ($2\nu_1 + \nu_8 \leftarrow \nu_8$) is clearly separated from the main absorption of the $2\nu_1$ band, and a similar large anharmonic coupling $x_{1,8}$ is expected as it has been found for $HCCCF_3$ and $HCCCH_3$.[73,74]

In the region of the second overtone of the CH-stretching vibration the bands of the alkylic and acetylenic chromophores are well separated by nearly 1000 cm^{-1}. They are shown for $HCCCH_2Cl$ and $HCCCH_2Br$ in Fig. 5. The spectrum for the alkylic vibration is spread over 400 cm^{-1} and is dominated by a strong band around 8550 cm^{-1}. The second overtone of the acetylenic CH-stretching vibration is located near 9700 cm^{-1} (see Fig. 5).

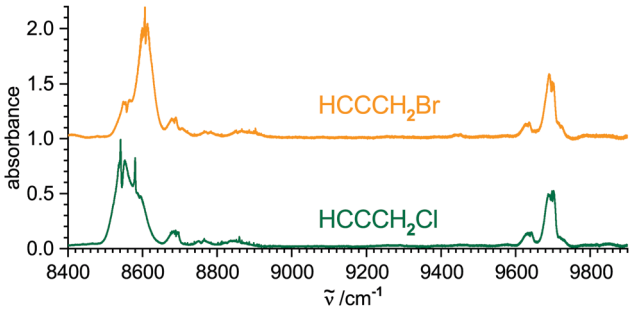

Fig. 5 IR-spectra for $HCCCH_2Cl$ (lower trace) and $HCCCH_2Br$ (upper trace) in the region of the second overtone measured with an instrumental bandwidth of 0.065 cm^{-1} on our FTIR-spectrometer (Bomem DA.002) with an absorption path length of 28 m and a gas pressure of 5 kPa.

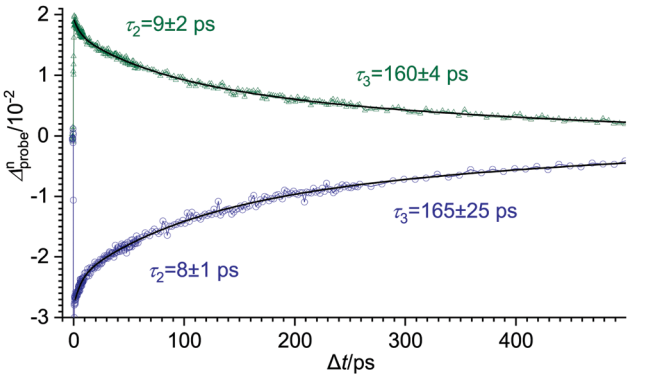

Fig. 6 Measured decay function with initial excitation of the CCH-chromophore in $HCCCH_2Cl$ with IR-probing. Two relaxation times τ_2 and τ_3 are obtained from a fit to the experimental data. A stimulated emission signal is obtained (upper trace) if the probe laser is tuned to $v_{CH} = 2 \rightarrow v_{CH} = 1$ transition. An absorption signal is measured for probing the $v_{CH} = 2 \rightarrow v_{CH} = 3$ transition.

3 Experimental results

3.1 Time resolved IR-probing of the initial decay of the CH chromophore excitation

The depopulation of the initially excited overtone of the CH-stretching vibration can be probed in the IR if the probe laser is tuned to the transition of $v_{CH} = 2$ to $v_{CH} = 3$ or to the transition of $v_{CH} = 1$ to $v_{CH} = 2$. In the first case an absorption signal is measured whereas in the latter case a stimulated emission signal is obtained. Additional spectroscopic information is necessary to measure the population of $v_{CH} = 1$ during the relaxation progress as the quantum removed from the CH-stretching vibration results in a population of lower frequency modes and thus includes a generally unknown anharmonic "hot band" shift of the absorption due to the off-diagonal anharmonicities $x_{CH,i}$ (with many possible i). Therefore, to obtain information about the population of $v_{CH} = 1$ the frequency of the probe beam has to be tuned in small steps around the $v_{CH} = 1$ to $v_{CH} = 2$ transition. For the excitation of the acetylenic CH-stretching vibration the transitions are well separated and are not overlapped by other transitions, the $v_{CH} = 1$ to $v_{CH} = 2$ transition at 3134 cm^{-1} and the $v_{CH} = 2$ to $v_{CH} = 3$ transition at 3229 cm^{-1}. The population of the $v_{CH} = 2$ vibrational level for the alkylic CH-stretching vibration could be probed at 2890 cm^{-1} for $HCCCH_2Cl$ and $HCCCH_2Br$ and at 2830 cm^{-1} for $HCCCH_2I$. An example for the relaxation kinetics of the acetylenic CH-stretching vibration in $HCCCH_2Cl$ is shown in Fig. 6 and the results for IR-probing are summarized in Table 1 together with the results for the UV probing.

For the initial relaxation of the alkylic CH-stretching vibration an upper limit of less than 1 ps is found (see Table 1). As can be seen from Fig. 6 an almost identical relaxation kinetics is obtained, independent whether the $v_{CH} = 2$ to $v_{CH} = 3$ transition at 3329 cm^{-1} is measured as absorption signal or the $v_{CH} = 2$ to $v_{CH} = 1$ transition at 3184 cm^{-1} in stimulated emission. From the almost identical time dependence for the two IR-probe frequencies it can be concluded that either the $v_{CH} = 1$ level is not significantly populated during the relaxation process or the absorption is shifted due to the anharmonic shift of the populated lower vibrational modes. For the IR-probing the depopulation of the initially excited CH-stretching vibration in the acetylenic chromophore had to be fitted with two decay times falling in the ranges $\tau_2 = 6$ to 9 ps and $\tau_3 = 40$ to 160 ps for all three molecules (see Table 1).

Table 1 Measured relaxation times for the propargyl halides. The numbers below the relaxation times give the relative contributions of the fast and slower process to the overall relaxation

Molecule	Excited vibr.	$\tilde{\nu}_{pump}$/ cm^{-1}	$\tilde{\nu}_{probe}$/ cm^{-1}	τ_1/ps	τ_2/ps	τ_3/ps
HC≡C–CH_2Cl	–CH_2Cl	5830	2899	<0.2	—	—
		5830	42 000	—	≤1.5	16 ± 2
					30%	70%
		5980	42 000	—	≤1.5	43 ± 7
					35%	65%
	HC≡C–	6562	3229	—	9 ± 2	160 ± 4
		6562	42 000	—	—	70 ± 9
HC≡C–CH_2Br	–CH_2Br	5880	2899	<0.4	—	—
		5880	36 000	—	2.5 ± 0.4	21 ± 2
					38%	62%
	HC≡C–	6562	3229	—	9 ± 2	135 ± 5
		6562	36 000	—	—	176 ± 25
HC≡C–CH_2I	–CH_2I	5880	2828	<0.7	—	—
		5880	29 400	—	<1.0	16 ± 5
					46%	54%
	HC≡C–	6562	3229	—	6 ± 1	44 ± 3
		6562	29 400	—	6 ± 2	35 ± 9
					47%	53%

3.2 Time resolved UV-detection of IVR in propargyl halides

For CH_3I it is known that the absorption to the different Q-states, showing at room temperature an absorption maximum around 260 nm, is shifted for vibrationally excited molecules to longer wavelengths.[51,52,75] It is well established that this shift is strongly correlated with the population of the CI-stretching vibration ν_3 and, to some extent, of the symmetric CH_3-umbrella mode ν_2. In the stimulated emission spectra of photodissociating CH_3I a progression of the CI-stretching vibration up to $v_3 = 9$ and of the CH_3-umbrella mode up to $v_2 = 2$ have been identified.[55] The measured spectra were exclusively explained taking only

into account combinations of these two vibrational modes. This explanation for the shift of the UV-absorption spectra was recently supported by *ab initio* calculations.[56] Based on a new potential surface for the electronically excited Q-states the absorption spectrum was calculated for different excitations of the CI-stretching vibration up to $v_3 = 2$. For molecules excited with two quanta in the CI-stretching vibration a maximum for the UV-absorption was predicted at 295 nm, shifted by 35 nm to longer wavelength as compared to the maximum for the molecules in the vibrational ground state.

There are only a few investigations available dealing with the UV-spectra of the propargyl halides. The absorption cross sections for $HCCCH_2Cl$ and $HCCCH_2Br$ between 160–280 nm have been published without giving any details about the configuration of the electronically excited states.[76] The UV-absorption shows an unstructured band with a constantly decreasing absorption cross section from 160 to 280 nm. The electronic structure has been studied for the propargyl chloride by resonance Raman spectroscopy and *ab initio* methods.[77] After excitation of $HCCCH_2Cl$ with a laser pulse at 199 nm a progression of the CCl-stretching vibration (ν_7 = 725 cm^{-1}) and the C≡C-stretching vibration (ν_3 = 2147 cm^{-1}) could be identified in the stimulated emission spectra, indicating a mixture of ππ*-, nσ*- and πσ*-contributions to the electronically excited state. The conclusions drawn from the emission spectra have been confirmed by the electronic structure obtained from *ab initio* calculations at the MP2/6-31G** level.[77] The electronic configuration derived is also consistent with the results from photodissociation experiments for $HCCCH_2Cl$ and $HCCCH_2Br$.[78] At an excitation wavelength of 193 nm a contribution of around 5% to the overall quantum yield was found for the channel leading to C_3H_2-radicals and HX (X = Cl, Br), whereas the main channel leads to elimination of the halogen atom. In more recent experiments on $HCCCH_2Cl$ an even higher yield of 10–20% has been found for this dissociation channel.[79] The reaction channel leading to HX-elimination could only be explained if ππ*-contributions are included in the configuration for the electronically excited state. To our knowledge no data are available dealing with the electronically excited states of $HCCCH_2I$, neither experimentally nor theoretically. However, one can draw some conclusions in analogy to the well known CH_3I.

In this part of our experiments the IVR process is detected through the shift of the UV-absorption spectrum to longer wavelengths. Considering the published results for $HCCCH_2Cl$ and $HCCCH_2Br$ a shift of the UV-absorption spectrum would indicate a population of the C≡C- and the CCl-stretching vibration. But one has to also take into account that for the expansion coefficients of the electronically excited state a strong dependence on the excitation energy is expected. The spectral region with a high ππ*-contribution may be estimated from the VUV-spectrum of propyne where nσ*- and πσ*-contributions, originating from the excitation at the halogen atom, are absent. There is no significant absorption cross section for longer wavelengths than 200 nm.[80] On the other hand the UV-absorption is extended more and more to longer wavelengths going from propargyl chloride to the iodide. These two circumstances led

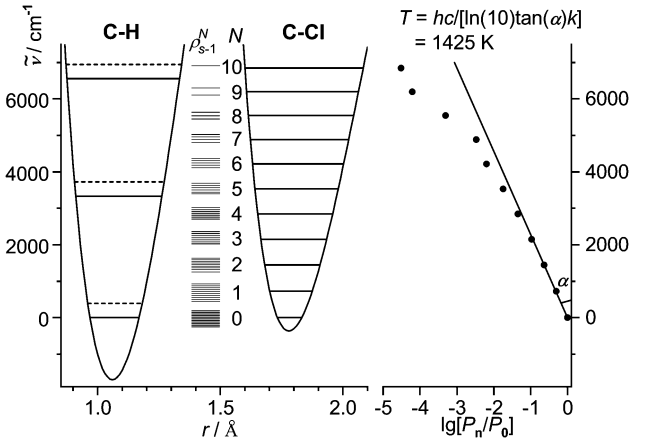

Fig. 7 Population distribution of the CCl-stretching mode in $HCCCH_2Cl$ for a microcanonical ensemble with an excitation energy of (*hc*)6952 cm^{-1}. The potential functions are shown schematically up to the excitation energy along the CH- and Cl-coordinate. The slope of the straight line fitted to the population function for small CCl-excitation energies gives an effective vibrational temperature of 1425 K for the microcanonical ensemble.

us to the assumption that the low frequency wings in the UV-absorption spectrum in the propargyl halides are dominated by the nσ*- and πσ*-components of the electronic states which are localized at the halogen atoms. And we conclude that the shift in the UV-spectra may be interpreted in the same manner as the one found in CH_3I. In consequence we assume that the measured probe signal in our experiments is related to the population of the CX-stretching vibration during the IVR process.

Fig. 7 shows as an example a schematic representation of the C–Cl-stretching vibrational levels and their calculated quasi-microcanonical distribution obtained after excitation of the CH-stretching overtone (see ref. 22). For the lower C–Cl-stretching levels this can be approximated by a Boltzmann distribution with T = 1425 K (see ref. 22 for a detailed discussion).

From our pump–probe experiments we cannot conclude whether a microcanonical equilibrium is reached after the end of the relaxation process or whether only a fraction of the energetically available phase space is covered. To be confident that a microcanonical distribution is reached, the population distributions for a number of vibrational modes would have to be measured. Here we assume that the excitation energy of E_{tot}/hc = 6952 cm^{-1} is given by the sum of the photon energy E_{phot}/hc = 6562 cm^{-1} and the thermal vibrational energy E_{300}/hc = 390 cm^{-1}. Also shown in the Fig. 7 are the vibrational levels of the acetylenic CH-stretching mode and the CCl-stretching mode in the anharmonic Morse oscillator approximation.

The normalized population for a single oscillator in equilibrium with a system of $m - 1$ coupled oscillators at an excitation energy E_n (n quanta in the CCl-stretching mode) is given by $P_n = \rho^{m-1}(E_{tot} - E_n)/\rho^{m-1}(E_{tot})$, where $\rho^{m-1}(E)$ is the vibrational density of states of m oscillators and the considered oscillator has been removed from the count.[22] From the initial slope of the population distribution an effective temperature of T_{eff} = 1425 K for the CCl-stretching vibration is calculated for

the microcanonical ensemble. This temperature is rather close to the vibrational temperature T_{therm} = 1310 K for a canonical ensemble with same total average vibrational energy corresponding to 6952 cm^{-1}.

3.3 Probing C–X stretching vibration after overtone excitation in propargyl halides

The UV-probe thus essentially detects the C–X stretching excitation by IVR. As the bandwidth of our pump laser is approximately 150 cm^{-1}, corresponding to our time resolution limits we can neither excite the complete alkyl Fermi-resonance polyad nor can the individual subbands of the alkylic CH-stretching vibration be excited separately. But it is possible to excite preferentially individual vibrations shifting the wavelength of the pump laser closer to one of the near-IR absorption bands or to the other. For $HCCCH_2Cl$ a slightly different decay kinetics was obtained for a preferential excitation of the weaker absorption band at 5980 cm^{-1}, as compared the excitation of the stronger band at 5830 cm^{-1}. Well separated from those overlapping bands is however the acetylenic CH-stretching vibration at 6570 cm^{-1}.

An example for a measured decay after the excitation of the CH_2X-group in $HCCCH_2Br$ is shown in Fig. 8. If the alkylic CH-stretching vibration is excited for any of the investigated propargyl halides, the decay processes can be fitted by a sum of two exponential functions with two different decay times τ_i, one fast decay process with $\tau_2 \leq 4$ ps and a slow decay process with τ_3 = 15–25 ps. We distinguish these from the fast initial decay τ_1, not observed in the UV-probe. A slightly slower relaxation with τ_3 = 42 ps was obtained if for $HCCCH_2Cl$ the laser wavelength is tuned to the weaker absorption band around 5975 cm^{-1}. An example for a measured decay in $HCCCH_2Cl$ for UV-probing is shown in Fig. 9. The relative contribution of the two different decay processes to the measured probe signal is approximately 1/3 for the faster process and 2/3 for the slower one. Extending the delay time for the UV-probe pulse up to 1 ns no indication for a slower decay process with $\tau > 100$ ps was found and we conclude that for the excitation of the CH_2X-group the IVR process is complete after 150–200 ps.

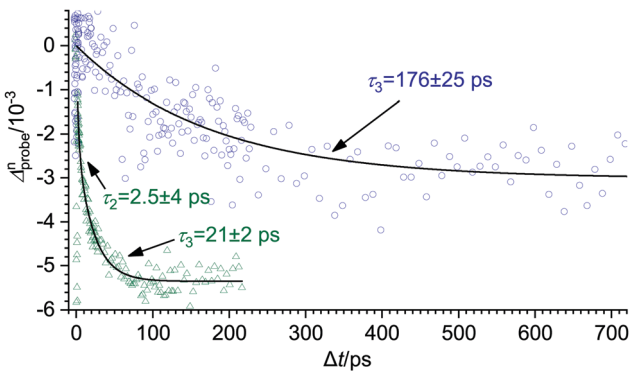

Fig. 8 Measured decay for the excitation in $HCCCH_2Br$ with UV-probing. For the excitation of the methylenic CH-stretching vibration two relaxation times τ_2 and τ_3 are obtained from a fit to the experimental data. For the excitation of the acetylenic CH-stretching vibration only a slow relaxation time τ_3 could be determined.

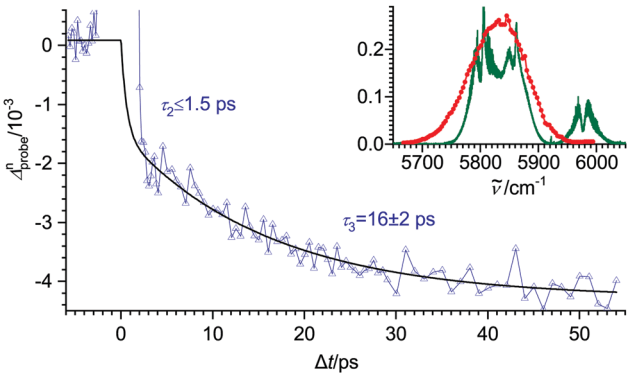

Fig. 9 Measured decay for the excitation of the alkylic CH-chromophore in $HCCCH_2Cl$ at 5830 cm^{-1}. Two relaxation times τ_2 and τ_3 are obtained from a fit to the experimental data. The inset shows the infrared absorption spectrum of the first overtone of the alkylic CH-stretching vibration with the emission spectrum of the pump laser superimposed.

If the relaxation were not complete and a long-lived non-statistical vibrational distribution were reached then at least for $HCCCH_2Cl$ and $HCCCH_2Br$, where a sample pressure of up to 3 kPa was used, a collisional IVR process would be expected, as it has been found in the pump–probe experiments on CH_3I.[52] From the fit to the experimental data the relaxation time τ_3 can be determined with satisfactory accuracy whereas for the fast relaxation time τ_2, especially if it is shorter than 2 ps, only an upper limit can be obtained, as the first 1–2 ps of our decay signals are heavily distorted by nonlinear effects arising from the temporal overlap of the pump and the probe pulse.

For the excitation of the acetylenic CH-stretching vibration in $HCCCH_2Cl$ and $HCCCH_2Br$ only one single slow relaxation time τ_3 = 70–200 ps has been found. An example for a measured decay process is shown in the upper part of Fig. 8. Within the accuracy of our experiment no indication for a faster relaxation process could be found, confirming the conclusion of a well isolated CCH-chromophore.

In the experiments with $HCCCH_2I$ for the excitation of the acetylenic CH-stretching vibration a faster transfer of the excitation to the C–X stretching vibration was observed, although not

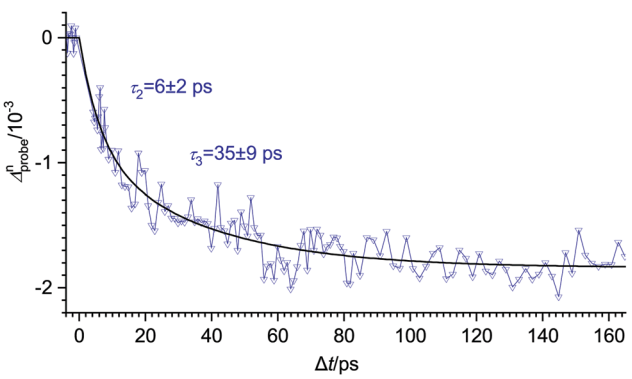

Fig. 10 Measured decay for the excitation of the CCH-chromophore in $HCCCH_2I$. Two relaxation times τ_2 and τ_3 are obtained from a fit to the experimental data.

quite as fast as for the initial excitation within the CH_2X-group. As can been seen from Fig. 10 a biexponential decay process was found with two different relaxation times $\tau_2 \leq 6$ ps and $\tau_3 \cong 35$ ps, indicating a significant coupling of the first overtone of the acetylenic CH-stretching vibration to the low frequency modes. For the excitation of both CH-stretching vibrations (acetylenic and alkylic) in $HCCCH_2I$ the fast and the slower relaxation processes contribute approximately equally to the total relaxation. The decay times, obtained for the different relaxation processes, are summarized in Table 1 together with the relative contributions of the different decay processes and the experimental parameters for the pump–probe experiments.

4 Discussion and conclusion

In the present work we have been able to study intramolecular vibrational energy flow in the "bichromophoric" molecules of the type $HCCCH_2X$ (with X = Cl, Br, I), which contain two spectrally well separated "infrared chromophores",[28] the alkylic sp^3 hybridized CH chromophore in the CH_2X group and the sp hybridized acetylenic $\equiv$C–H chromophore. Excitation in the spectral ranges of the first overtone of these chromophores with 150 fs laser pulses of different frequency allows one to separately excite these chromophores. The subsequent vibrational energy flow has been probed by two different techniques

(i) Probing the infrared absorption or stimulated emission out of the second overtone level allowed us to obtain information of the decay of the initial excitation in either of the two chromophores.

(ii) Probing the UV absorption allowed us to study the arrival of the vibrational energy in the C–X vibrations.

The main results of this investigation are summarized in Table 1. When exciting the alkylic CH chromophore, there is a very fast initial energy loss of CH-stretching vibrational energy (τ_1), faster than our time resolution of 150 fs, in agreement with the Fermi-resonance doorway established from numerous spectroscopic studies of the alkylic CH chromophore.[28] In addition, the UV probing indicates the arrival of this vibrational energy in the CX vibrations, which is characterized by a biexponential kinetics. There is firstly a fast initial part with times τ_2 in the range 1 to 3 ps contributing between about 30 and 50% of the signal (depending on the molecule) and secondly a slower part with times τ_3 in the range 15 to 20 ps contributing between about 70 and 50%. Not unexpectedly the transfer of the energy from alkyl CH stretching to the CX vibrations is thus a more complex process, for which several possible mechanisms can be advanced, which we do not distinguish in our current experiments. In order to unravel these in more detail, either a probing of excitation in other, intermediate modes would be required or a complete high-resolution analysis of the full-dimensional quantum dynamics, which is at the limit of current possibilities.[81]

When we excite initially the acetylenic $\equiv$C–H chromophore, we find a very different behavior (Table 1). The decay from the initial CH-stretching vibration probed in the infrared has no ultrafast subpicosecond contribution τ_1. It is characterized by a biexponential behaviour with time τ_2 in the range 5 to 10 ps (depending on the molecule) and a dominant τ_3 in the range 40 to 160 ps. This slow initial decay from the $\equiv$C–H chromophore excitation is again in perfect agreement with the earlier conclusions derived for this chromophore from high resolution spectroscopic studies[23,28,29] and this answers some of the questions raised some time ago on the comparison of results from these two very different approaches.[37,38] Furthermore, UV probing also indicates a slow arrival of vibrational energy in the CX vibrations, when exciting the acetylenic $\equiv$C–H chromophore. For $HCCCH_2Cl$ and $HCCCH_2Br$ only one slow exponential decay time is apparent with $\tau_3 = 70$ ps and 176 ps, respectively, although we would not be able to exclude a closer superposition of several exponentials. For $HCCCH_2I$ the behaviour is significantly different, as we find a biexponential behaviour with quite a fast contribution $\tau_2 = 6$ ps (also seen in the IR probing of this molecule) and $\tau_3 \simeq 40$ ps, also similar in both the IR and the UV probing of this molecule. This might indicate some specific coupling of $2\nu_1$ in the propargyl iodide to a state which we suspect to be a combination of a CH_2 stretching overtone ($2\nu_2$ or $2\nu_{11}$, A′) with a CI-stretching vibration (ν_7, A′) which would fall in the range 6600 to 6620 cm^{-1}, close to $2\nu_1$ ($\sim$6560 cm^{-1}). This question deserves further study by high resolution spectroscopy. The bichromophoric systems would also be of interest for studies at higher time resolution including attosecond spectroscopy.[82–85] In any case the overall picture of intramolecular vibrational redistribution processes in these interesting bichromophoric molecules as derived from our femtosecond pump–probe kinetic spectroscopy is consistent with the general results derived from high resolution spectroscopy showing very distinct behaviour of two functional groups, the alkyl CH chromophore and the acetylenic CH chromophore.[28]

Conflicts of interest

There are no conflicts to declare.

Acknowledgements

The initial experiments of our work have profited from many discussions with Vitaly Krylov, to whose memory this paper is dedicated. We received important technical support from Fabienne Arn, Guido Grassi, Eduard Peyer, Andreas Schneider, Reto Ulrich, and Daniel Zindel in our laboratory. We also enjoyed help from and discussions with Sieghard Albert, Irina Bolotova, Olga Gromova, Ľuboš Horný, Veronika Horka-Zelenkova, Fabio Mariotti, Carine Manca Tanner, Frederic Merkt, Hans-Martin Niederer, Robert Prentner, Martin Suter, Fatih Ünlü and Hans Jakob Wörner, as well as correspondence with Helmut Schwarz. Our work was supported financially by the ETH Zürich, the Schweizerischer Nationalfonds and some current support from the COST project MOLIM (molecules in motion).

References

1 H. Eyring, *J. Chem. Phys.*, 1935, **3**, 107–115.

2 R. A. Marcus and O. K. Rice, *J. Phys. Colloid Chem.*, 1951, **55**, 894–908.
3 B. S. Rabinovitch and J. D. Rynbrandt, *J. Phys. Chem.*, 1997, **75**, 2164–2171.
4 W. L. Hase, *J. Chem. Phys.*, 1972, **57**, 730–733.
5 M. Quack and J. Troe, *Ber. Bunsen-Ges. Phys. Chem.*, 1974, **78**, 240–252.
6 M. Quack and J. Troe, in *Gas Kinetics and Energy Transfer*, ed. P. Ashmore and R. J. Donovan, The Chemical Society, London, 1977, vol. 2, pp. 175–238.
7 M. Quack and J. Troe, in *Theoretical chemistry: Advances and perspectives (Theory of scattering, papers in honor ofHenry Eyring)*, ed. D. Henderson, Academic Press, New York, 1981, vol. 6B, pp. 199–276.
8 M. Quack and J. Troe, *Int. Rev. Phys. Chem.*, 1981, **1**, 97–147.
9 M. J. Pilling and I. W. M. Smith, *Modern Gas Kinetics: Theory, Experiment and Applications*, Blackwell Scientific Publications, Oxford, 1987.
10 M. Quack and J. Troe, in *Encyclopedia of Computational Chemistry*, John Wiley and Sons, 1998, vol. 4, pp. 2708–2726.
11 A. S. Sudbo, P. A. Schulz, E. R. Grant, Y. R. Shen and Y. T. Lee, *J. Chem. Phys.*, 1978, **68**, 1306–1307.
12 M. Quack, *J. Chem. Phys.*, 1978, **69**, 1282–1307.
13 M. Quack and G. Seyfang, *J. Chem. Phys.*, 1982, **76**, 955–965.
14 M. Quack and E. Sutcliffe, *Chem. Phys. Lett.*, 1984, **105**, 147–152.
15 D. W. Lupo and M. Quack, *Chem. Rev.*, 1987, **87**, 181–216.
16 M. Quack, *Infrared Phys.*, 1989, **29**, 441–466.
17 M. Quack, *Infrared Phys. Technol.*, 1995, **36**, 365–380.
18 R. Marquardt and M. Quack, in *Encyclopedia of Chemical Physics and Physical Chemistry*, IOP publishing, Bristol, 2001, vol. 1 (Fundamentals), ch. A. 3.13, pp. 897–936.
19 M. Shapiro and P. Brumer, *Principles of the Control of Molecular Processes*, John Wiley & Sons, New York, 2003.
20 E. Fermi, *Z. Phys.*, 1931, **71**, 250–259.
21 G. Herzberg, *Infrared and Raman Spectra of Polyatomic Molecules*, D. Van Nostrand, New York, 1945.
22 M. Quack, *Nuovo Cimento B*, 1981, **63**, 358–377.
23 K. von Puttkamer, H. R. Dübal and M. Quack, *Faraday Discuss. Chem. Soc.*, 1983, **75**, 197–210.
24 H. R. Dübal and M. Quack, *J. Chem. Phys.*, 1984, **81**, 3779–3791.
25 H. R. Dübal and M. Quack, *Mol. Phys.*, 1984, **53**, 257–264.
26 R. Marquardt, M. Quack, J. Stohner and E. Sutcliffe, *J. Chem. Soc., Faraday Trans. 2*, 1986, **82**, 1173–1187.
27 J. Segall, R. N. Zare, H. R. Dübal, M. Lewerenz and M. Quack, *J. Chem. Phys.*, 1987, **86**, 634–646.
28 M. Quack, *Annu. Rev. Phys. Chem.*, 1990, **41**, 839–874.
29 B. H. Pate, K. K. Lehmann and G. Scoles, *J. Chem. Phys.*, 1991, **95**, 3891–3916.
30 M. Quack and J. Stohner, *J. Phys. Chem.*, 1993, **97**, 12574–12590.
31 M. Quack, *J. Mol. Struct.*, 1995, **347**, 245–266.
32 M. Quack, in *Femtosecond Chemistry, Molecular femtosecond quantum dynamics between less than yoctoseconds and more than days: Experiment and theory*, ed. J. Manz and L. Wöste, Verlag Chemie, Weinheim, 1995, ch. 27, pp. 781–818.
33 M. Quack and W. Kutzelnigg, *Ber. Bunsen-Ges. Phys. Chem.*, 1995, **99**, 231–245.
34 M. Quack, *Chimia*, 2001, **55**, 753–758.
35 Y. B. He, J. Pochert, M. Quack, R. Ranz and G. Seyfang, *Faraday Discuss. Chem. Soc.*, 1995, **102**, 275–300.
36 A. H. Zewail, in *Femtosecond Chemistry, Femtochemistry: Concepts and Applications*, ed. J. Manz and L. Wöste, Verlag Chemie, Weinheim, 1995, ch. 2, pp. 15–128.
37 M. Quack, *Adv. Chem. Phys.*, 1997, **101**, 83–84, 92–93, 202, 277–278, 282, 373–388, 443, 453–456, 459, 586–591, 595.
38 R. A. Marcus, *Adv. Chem. Phys.*, 1997, **101**, 391.
39 H. J. Bakker, P. C. M. Planken and A. Langendijk, *J. Chem. Phys.*, 1991, **94**, 6007–6013.
40 P. Hamm, M. Lim and R. M. Hochstrasser, *J. Chem. Phys.*, 1997, **107**, 10523–10531.
41 R. Laenen and K. Simeonidis, *Chem. Phys. Lett.*, 1999, **299**, 589–596.
42 V. Kozich, W. Werncke, J. Dreyer, K. Brzezinka, M. Rini, A. Kummrow and T. Elsaesser, *J. Chem. Phys.*, 2002, **117**, 719–726.
43 H. Yoo, M. DeWitt and B. Pate, *J. Phys. Chem. A*, 2004, **108**, 1348–1364.
44 W. Kaiser, *Ber. Bunsen-Ges. Phys. Chem.*, 1985, **89**, 213–217.
45 F. Emmerling, M. Lettenberger and A. Laubereau, *J. Phys. Chem.*, 1996, **100**, 19251–19256.
46 D. Bingemann, M. P. Gorman, A. M. King and F. F. Crim, *J. Chem. Phys.*, 1997, **107**, 661–664.
47 D. Bingemann, A. M. King and F. F. Crim, *J. Chem. Phys.*, 2000, **113**, 5018–5025.
48 A. Charvat, J. Assmann, B. Abel and D. Schwarzer, *J. Phys. Chem. A*, 2001, **105**, 5071–5080.
49 J. Assmann, M. Kling and B. Abel, *Angew. Chem., Int. Ed.*, 2003, **42**, 2226–2246.
50 D. Schwarzer, C. Hanisch, P. Kutne and J. Troe, *J. Phys. Chem. A*, 2002, **106**, 8019–8028.
51 C. G. Elles, M. J. Cox and F. F. Crim, *J. Chem. Phys.*, 2004, **120**, 6973–6979.
52 V. Krylov, M. Nikitchenko, M. Quack and G. Seyfang, in Nonlinear Frequency Generation and Conversion: Materials, Devices and Applications III, Proc. SPIE, Bellingham, WA, 2004, vol. 5337, pp. 178–189.
53 T. Ebata, M. Kayano, S. Sato and N. Mikami, *J. Phys. Chem. A*, 2001, **105**, 8623–8628.
54 Y. Yamada, N. Kayano, N. Mikami and T. Ebata, *J. Chem. Phys.*, 2005, **123**, 124316.
55 R. Sundberg, D. Imre, M. Hale, J. Kinsey and R. D. Coalson, *J. Phys. Chem.*, 1986, **90**, 5001–5009.
56 A. Alekseyev, H. Liebermann, R. Buenker and S. Yurchenko, *J. Phys. Chem.*, 2007, **126**, 234102.
57 H. S. Yoo, M. J. DeWitt and B. H. Pate, *J. Phys. Chem. A*, 2004, **108**, 1348–1364.
58 H. S. Yoo, M. J. DeWitt and B. H. Pate, *J. Phys. Chem. A*, 2004, **108**, 1365–1379.
59 H. S. Yoo, D. A. McWorther and B. H. Pate, *J. Phys. Chem. A*, 2004, **108**, 1380–1387.
60 A. L. Malinovsky, A. A. Makarov and E. Ryabov, *J. Exp. Theor. Phys.*, 2008, **106**, 34–45.

61 A. L. Malinovsky, A. A. Makarov and E. Ryabov, *JETP Lett.*, 2011, **93**, 124–128.
62 A. L. Malinovsky, A. A. Makarov and E. Ryabov, *Phys. Scr.*, 2012, **85**, 058102.
63 V. Krylov, A. Kushnarenko, E. Miloglyadov, M. Quack and G. Seyfang, in Commercial and Biomedical Applications of Ultrafast Lasers VII, (Proceedings, Photonics West 2007; 20–25 Jan 2007, San Jose California), Proceedings of SPIE Volume 6460, 2007, p. 64601D-1.
64 A. Kushnarenko, V. Krylov, E. Miloglyadov, M. Quack and G. Seyfang, in Ultrafast Phenomena XVI, Proceedings of the 16th International Conference on Ultrafast Phenomena, Stresa, Italia, June 2008, Springer, Berlin, 2009, vol. 92, pp. 349–351.
65 V. Krylov, A. Kushnarenko, E. Miloglyadov, M. Quack and G. Seyfang, *Chimia*, 2008, **62**, 668.
66 A. Kushnarenko, E. Miloglyadov, M. Quack and G. Seyfang, *Faraday Discuss. Chem. Soc.*, 2011, **150**, 520–521.
67 E. A. J. Marcatili and R. A. Schmeltzer, *Bell. Syst. Tech. J.*, 1964, **43**, 1783–1809.
68 R. K. Nubling and J. A. Harrington, *Opt. Eng.*, 1998, **37**, 2454–2458.
69 T. Pfeifer and M. Downer, *J. Opt. Soc. Am. B*, 2007, **24**, 1025–1029.
70 C. S. L. Baker, P. D. Landor, S. R. Landor and A. N. Patel, *J. Chem. Soc.*, 1965, 4348.
71 J. Evans and R. Nyquist, *Spectrochim. Acta*, 1963, **19**, 1153–1163.
72 O. Saur, J. Travert, J. Lavalley and N. Sheppard, *Spectrochim. Acta, Part A*, 1973, **29**, 243–252.
73 H. R. Dübal and M. Quack, *Chem. Phys. Lett.*, 1982, **90**, 370–374.
74 A. Campargue, A. Biennier, A. Garnache, A. Kachanov, D. Romanini and M. Herman, *Ann. Phys.*, 1999, **111**, 7888–7903.
75 A. Charvat, J. Assmann, B. Abel, D. Schwarzer, K. Henning, K. Luther and J. Troe, *Phys. Chem. Chem. Phys.*, 2001, **3**, 2230–2240.
76 A. Fahr, P. Hassanzadeh, B. Laszlo and R. Huie, *Chem. Phys.*, 1997, **215**, 59–66.
77 P. Browning, D. Kitchen and L. Butler, *J. Phys. Chem.*, 1996, **100**, 7765–7771.
78 Y. Lee and S. Lin, *J. Chem. Phys.*, 1998, **108**, 134–141.
79 L. McCunn, D. Bennett, L. Butler, H. Fan, F. Aguirre and S. Pratt, *J. Phys. Chem. A*, 2006, **110**, 843–850.
80 F. Chen, D. Judge and C. Wu, *Chem. Phys.*, 2000, **260**, 215–223.
81 S. Albert, E. Bekhtereva, I. Bolotova, Z. Chen, C. Fàbri, H. Hollenstein, M. Quack and O. Ulenikov, *Phys. Chem. Chem. Phys.*, 2017, **19**, 26527–26534.
82 H. J. Wörner and P. B. Corkum, *Handbook of High Resolution Spectroscopy*, Wiley, Chichester, New York, 2011, vol. 2, ch. 15, pp. 1781–1803.
83 A. Tehlar and H. J. Wörner, *Mol. Phys.*, 2013, **111**, 2057–2067.
84 P. M. Kraus, P. M. Mignolet, D. Baykusheva, A. Rupenyan, L. Horny, E. F. Penka, G. Grassi, O. I. Tolstikhin, J. Schneider, F. Jensen, L. B. Madsen, A. D. Bandrauk, F. Remacle and H. J. Wörner, *Science*, 2015, **355**, 790–795.
85 Y. Pertot, C. Schmidt, M. Matthews, A. Chauvet, M. Huppert, V. Svoboda, A. von Conta, A. Tehlar, D. Baykusheva, J. P. Wolf and H. J. Wörner, *Science*, 2017, **355**, 264–267.